

The leaders profile method: detection of distinct processes in a signal

Thomas KLEYNTSSENS, Samuel NICOLAY

Université de Liège, Institut de Mathématique (B37), Quartier Polytech 1, allée de la Découverte 12, B-4000 Liège, Belgium.

tkleyntssens@ulg.ac.be, s.nicolay@ulg.ac.be

Résumé – La méthode du profil des coefficients dominants est un formalisme multifractal permettant d’obtenir des spectres non nécessairement concaves ou croissants. Notre algorithme peut détecter la présence de processus distincts dans un même signal. Nous présentons ici les premiers résultats obtenus.

Abstract – The leaders profile method is a multifractal formalism that allows to compute non-concave and non-increasing spectra. Our implementation can detect the presence of distinct processes in a signal. We present here the first results obtained.

1 Introduction

We present a new approach to study the pointwise regularity of signals. Let us recall some usual concepts.

Definition 1 *Let $f : \mathbf{R}^n \rightarrow \mathbf{R}$ be a locally bounded function and $x_0 \in \mathbf{R}^n$; f belongs to the Hölder space $\Lambda^\alpha(x_0)$ (with $\alpha \geq 0$) if there exist a constant $C > 0$ and a polynomial P of degree less than α such that*

$$|f(x) - P(x)| < C|x - x_0|^\alpha \quad (1)$$

in a neighborhood of x_0 . As usual, a function f belongs to $\Lambda^\alpha(\mathbf{R}^n)$ if f belongs to $\Lambda^\alpha(x_0)$ for any x_0 , the constant C in (1) being uniform.

A notion of regularity of f at x_0 is given by the Hölder exponent of f at x_0 ; it is defined by

$$h_f(x_0) = \sup\{\alpha \geq 0 : f \in \Lambda^\alpha(x_0)\}.$$

Computing this exponent is very difficult and sometimes impossible. It is easier to get a global information about the pointwise regularity using the notion of the Hölder spectrum function.

Definition 2 *The Hölder spectrum of a function f is the function*

$$\begin{aligned} d_f : [0, +\infty] &\rightarrow \{-\infty\} \cup [0, n], \\ h &\mapsto \dim_{\mathcal{H}} \{x \in \mathbf{R}^n : h_f(x) = h\}, \end{aligned}$$

where $\dim_{\mathcal{H}}$ is the Hausdorff dimension.

Computing the Hölder spectrum by directly using the definition given above is impossible in most of the practical cases, but there exist heuristic methods to estimate d_f that give satisfactory results in many situations. A method was first proposed by Parisi and Frisch [14]; later, Arneodo et al. proposed a similar method based on the continuous wavelet transform [2].

In both approaches, the decreasing part of the spectrum cannot be obtained. To take care of this problem, Arneodo et al. proposed the wavelet transform modulus maxima (WTMM) method [13], using the notion of line of maxima in the wavelet transform. This technique proved helpful in many practical problems, but in theory, it cannot be linked to a functional space. This is why Jaffard replaced the continuous wavelet transform with the discrete one and introduced the wavelet leaders method (WLM) [9, 10]. When comparing the WTMM with the WLM, numerical results are similar [11], but the WLM allows to obtain an upper bound of the Hölder spectrum of f if $f \in \Lambda^\alpha(\mathbf{R}^n)$ for some $\alpha > 0$ [9].

In the methods presented above, the spectrum is obtained by applying an inverse Legendre transform and so is necessarily concave. However, it is possible to compute functions whose spectrum is not concave. To overcome this second problem, Jaffard introduced a multifractal formalism based on the so-called S^ν spaces [8], whose definition involves discrete wavelet coefficients. This method has been implemented and allows to effectively recover non-concave spectra [12]. But the problem encountered with the first approaches reappears: one cannot access the decreasing part of the spectrum through the S^ν spaces. To tackle this, the idea is to replace the wavelet coefficients in the definition of S^ν with the wavelet leaders. These new spaces are called L^ν spaces [4]. By doing so, one defines a new multifractal formalism that leads to the detection of non-increasing and non-concave spectra, called the leaders profile method (LPM). From a theoretical point of view, this new approach is better than the previous methods [6] and it is complementary to the WLM in practice [1, 6].

In section 2, we recall the notion of wavelet leader and we give an implementation of the LPM. In section 3, we present the LPM on several numerical examples, and we show that our implementation allows a more precise study of a signal compared to other methods; we can detect the coexistence of two processes in a signal.

2 The leaders profile method

2.1 The discrete wavelet transform and the wavelet leaders

Under some general assumptions [5], there exist a function ϕ and $2^n - 1$ functions $(\psi^{(i)})_{1 \leq i < 2^n}$, called wavelets, such that for any $f \in L^2(\mathbf{R}^n)$, we have

$$f(x) = \sum_{k \in \mathbf{Z}^n} C_k \phi(x - k) + \sum_{j \in \mathbf{N}} \sum_{k \in \mathbf{Z}^n} \sum_{1 \leq i < 2^n} c_{j,k}^{(i)} \psi^{(i)}(2^j x - k),$$

where

$$c_{j,k}^{(i)} = 2^{nj} \int_{\mathbf{R}^n} f(x) \psi^{(i)}(2^j x - k) dx$$

and

$$C_k = \int_{\mathbf{R}^n} f(x) \phi(x - k) dx.$$

On the torus $\mathbf{R}^n / \mathbf{Z}^n$, we will use the periodized wavelets

$$\psi_p^{(i)}(2^j x - k) = \sum_{l \in \mathbf{Z}^n} \psi^{(i)}(2^j(x - l) - k)$$

to form a basis of the one periodic functions on \mathbf{R}^n which locally belong to $L^2(\mathbf{R}^n)$. The corresponding coefficients $c_{j,k}^{(i)}$ are naturally called the periodized wavelet coefficients. In the sequel, we will use another notation, more practical, for the wavelet coefficients. We denote by $\lambda_{j,k}^{(i)}$ the dyadic cube

$$\lambda_{j,k}^{(i)} = \frac{i}{2^{j+1}} + \frac{k}{2^j} + [0, \frac{1}{2^{j+1}})^n.$$

We will omit any reference to the indices i, j and k for such cubes by writing $\lambda = \lambda_{j,k}^{(i)}$. The set Λ_j will denote the set of dyadic cubes λ of $[0, 1]^n$ with side 2^{-j} and the wavelet coefficient $c_{j,k}^{(i)}$ will be denoted by c_λ .

The wavelet leader associated to the cube λ is the quantity

$$d_\lambda = \sup_{\lambda' \subset 3\lambda} |c_{\lambda'}|.$$

2.2 Implementation of the LPM

The LPM provides an approximation of the Hölder spectrum of f given by [4]

$$\tilde{d}_f^C(h) = \begin{cases} \lim_{\epsilon \rightarrow 0^+} \limsup_{j \rightarrow +\infty} \frac{\log \#E_j^>(C, h + \epsilon)}{\log 2^j} & \text{if } h \leq h_s \\ \lim_{\epsilon \rightarrow 0^+} \limsup_{j \rightarrow +\infty} \frac{\log \#E_j^<(C, h - \epsilon)}{\log 2^j} & \text{if } h \geq h_s \end{cases} \quad (2)$$

where $E_j^\vartheta(C, h) = \{\lambda \in \Lambda_j : d_\lambda \vartheta C 2^{-hj}\}$ ($\vartheta \in \{\leq, \geq\}$), C is a constant strictly positive and h_s is the smallest positive number such that the function of the first line of (2) is equal to n . The constant C appearing in (2) is arbitrary, i.e $\tilde{d}_f^C = \tilde{d}_f^{C'}$ for any $C, C' > 0$ [6], and it is usually equal to 1. We denote \tilde{d}_f^1 by \tilde{d}_f and it is called the leaders profile of f . We also set by $h_{\min} = \inf\{h : \tilde{d}_f(h) \geq 0\}$ and $h_{\max} = \sup\{h : \tilde{d}_f(h) \geq 0\}$. It can be shown that the leaders profile does not depend on the chosen wavelet basis [4].

The definition of $\tilde{d}_f^C(h)$ formalizes the idea that, if $h \in [h_{\min}, h_s]$ (resp. $h \in [h_s, h_{\max}]$), there are about $2^{\tilde{d}_f^C(h)j}$ wavelet leaders larger (resp. smaller) than $C 2^{-hj}$ for j “large enough”. So, it is natural to approximate $\tilde{d}_f^C(h)$ by the slope of

$$j \mapsto \frac{\log \#E_j^>(C, h)}{\log 2} \quad (\text{resp. } j \mapsto \frac{\log \#E_j^<(C, h)}{\log 2}) \quad (3)$$

for j “large enough” if $h \in [h_{\min}, h_s]$ (resp. $h \in [h_s, h_{\max}]$). In practice, we fix a threshold for the correlation of the points used to compute the slope: we only keep the points associated to a correlation coefficient higher than the threshold. The impact of the choice of this threshold has been studied in [6]. From now on, the notation $\tilde{d}_f^C(h)$ will refer to this slope.

To determine the value of h_s , we proceed as follows: we begin with h equal to 0 and use $E_j^>(C, h)$ to approximate $\tilde{d}_f(h)$. We then increase h until the detected value of $\tilde{d}_f(h)$ is close to n . The estimated value of h_s will be equal to this last h and for larger h , we use $E^<(C, h)$.

To compute an approximation of $\tilde{d}_f(h)$ using the values $\tilde{d}_f^C(h)$, it is important to understand that the main difference between theory and practice lies in the choice of the constant C in $\tilde{d}_f^C(h)$. In theory, the constant can be chosen arbitrarily. It is not true in practice because we only have access to a finite number of wavelet leaders. If the typical value of wavelet leaders is too large (resp. too small) with respect to C , too many (resp. not enough) of them will be taken into account, so that the value $\tilde{d}_f^C(h)$ will be very different from the theoretical value $\tilde{d}_f(h)$.

Consequently, for a fixed $h > 0$, we construct the function

$$C > 0 \mapsto \tilde{d}_f^C(h)$$

to approximate the value of $\tilde{d}_f(h)$. If $h \leq h_s$ (resp. $h > h_s$) this function should be decreasing (resp. increasing). If $h \in [h_{\min}, h_{\max}]$, it should exist an interval I for which the values $\tilde{d}_f^C(h)$ with $h \in I$ are close from each other. We take the mean of these values as an approximation of $\tilde{d}_f(h)$ and use a gradient descent to detect this interval [12, 6].

3 Numerical simulations

The efficiency of the implementation described in the previous section has already been presented in [6]. It has been shown that the function

$$C > 0 \mapsto \tilde{d}_f^C(h)$$

allows to approximate the Hölder spectrum of f in h . In this section, we show that this function can give some additional information about the signal. This fact has been discovered during the study of the binomial cascade after a thresholding.

Definition 3 *The binomial cascade of parameter $p \in (0, 1)$ is the only Borel measure μ defined on $[0, 1]$ such that*

$$\mu\left(\left[\sum_{k=1}^n \frac{\epsilon_k}{2^k}, \sum_{k=1}^n \frac{\epsilon_k}{2^k} + \frac{1}{2^n}\right)\right) = p^{\sum_{k=1}^n \epsilon_k} (1-p)^{n - \sum_{k=1}^n \epsilon_k},$$

for all $n \in \mathbf{N}$ and $\epsilon_k \in \{0, 1\}$ ($k \in \{1, \dots, n\}$).

The method of *threshold of order* $\gamma > 0$ consists in replacing the wavelet coefficients c_λ by $c_\lambda^t = c_\lambda \mathbf{1}_{|\cdot| \geq 2^{-\gamma j}}(c_\lambda)$. In Figure 1, we illustrate the spectrum of a binomial cascade after a thresholding. It is non-concave [16].

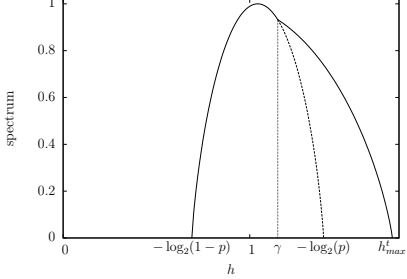


Figure 1: Comparaison between the spectrum of a binomial cascade of parameter $p = 0.38$ (dotted black) and its threshold of order $\gamma = 1.15$

In Figure 2, several examples of functions $C > 0 \mapsto \tilde{d}_f^C(h)$ are represented for different values of h . Recall that in order to compute $d_f^C(h)$, we use the approximation of the increasing part of the spectrum, i.e. the first function defined by (3).

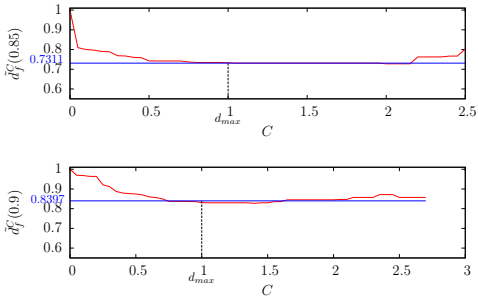


Figure 2: Function $C \mapsto \tilde{d}_f^C(h)$ where $h = 0.85$ (above) and $h = 0.9$ (below) for the increasing part of the spectrum of a cascade of parameter $p = 0.38$ with a threshold of order $\gamma = 1.15$

While studying the function $C \mapsto \tilde{d}_f^C(h)$ with $h > \gamma$ for the approximation of the decreasing part of the threshold cascade, i.e. the second function defined by (3), we have noticed two stabilizations. The highest corresponds to the theoretical value, while the smallest corresponds to the cascade without the threshold. In Figure 3, several examples are represented.

The presence of two stabilizations can be explained as a numerical phenomenon. The threshold replaces the small coefficients by 0. So, the value of $d_f^C(h)$ (recall that it depends on the number of coefficients smaller than $C2^{-hj}$) for small C reflects this modification. On the opposite, the value of $d_f^C(h)$ for large C is less affected by this change and allows to detect the presence of the original cascade.

The theoretical spectra of a binomial cascade with a threshold are compared with the spectra obtained by LPM and WLM in Figure 4. The different values of the second stabilization are

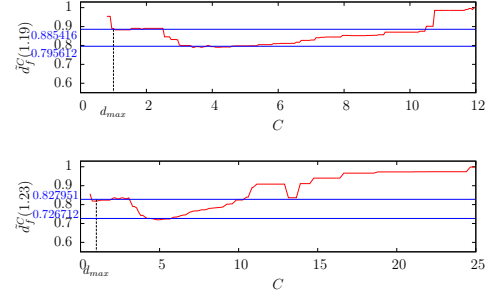


Figure 3: Function $C \mapsto \tilde{d}_f^C(h)$ where $h = 1.19$ (above) and $h = 1.23$ (below) for the decreasing part of the spectrum of a cascade of parameter $p = 0.38$ with a threshold of order $\gamma = 1.15$

also represented. We see that LPM underestimates the theoretical spectrum but detects the non-concave part of the spectrum of the threshold function and sees the presence of the original cascade. WLM does not detect this non-concave part.

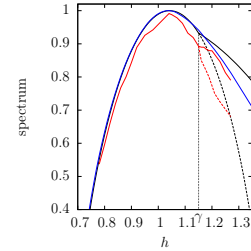


Figure 4: Spectrum of a cascade of parameter $p = 0.38$ with a threshold of order $\gamma = 1.15$. Black (resp. red and blue) theoretical spectrum (resp. LPM and WLM). Dotted black (resp. red) theoretical spectrum of a cascade of parameter $p = 0.38$ (resp. the smallest stabilization detected with LPM)

Now, let us study a Lévy process. It is a stochastic process with independent and stationary increments that is right-continuous and admits almost surely a left limit at all points. It is for example used in the field of financial modeling [15]. Any Lévy process can be decomposed into the sum of a (possibly vanishing) Brownian part and an independent pure jumps process. In this work, we study a Lévy process with a Brownian part. Recall that a Lévy process is associated to an index $\beta \in [0, 2]$, called the *Blumenthal and Getoor lower index*, that governs the multifractal properties of the process [7]. More precisely, if the process has a Brownian part, the associated Hölder spectrum is non-concave and, almost surely, is equal to

$$d_f(h) = \begin{cases} \beta h & \text{if } h \in [0, 1/2] \\ 1 & \text{if } h = 1/2 \end{cases} .$$

To simulate a Lévy process with a Brownian part, we create a Lévy process without Brownian part and a Brownian motion is then added. In Figure 5, we have represented the function $C \mapsto \tilde{d}_f^C(h)$ for the approximation of the increasing part of the spectrum. For $h \leq 0.5$, we only see the Lévy process. For

$h > 0.5$, there are two stabilizations, corresponding to one of the processes used to construct the signal: the Lévy process without Brownian part and the Brownian motion. The highest stabilization corresponds to the theoretical value. Moreover, the smallest stabilization corresponds to the Lévy process without Brownian part.

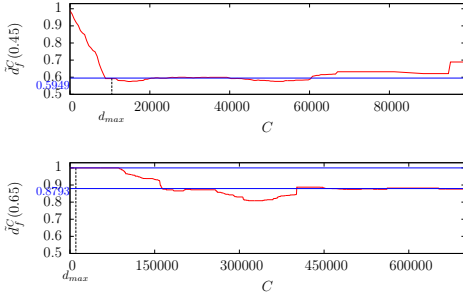


Figure 5: Functions $C \mapsto \tilde{d}_f^C(h)$ with $h = 0.45$ (above) and $h = 0.65$ (below) for a Lévy process with a Brownian part ($\beta = 1.3$)

In Figure 6, the theoretical spectrum is compared with the spectrum obtained with LPM and WLM. The smallest stabilization is also represented for $h > 0.5$. First, we see that the WLM tends to determine a strictly concave spectrum while LPM fit the theoretical spectrum better. Secondly, the spectrum of the Lévy process without Brownian part used to simulate the Lévy process with a Brownian part is detected.

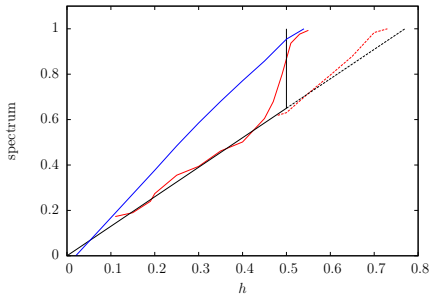


Figure 6: Spectrum of a Lévy process with a Brownian part ($\beta = 1.3$). Black (resp. red and blue) theoretical (resp. LPM and WLM) spectrum. Dotted red the detection of the spectrum of the associated Lévy process without Brownian part. The results are obtained on 50 simulations of size 2^{20}

4 Conclusion

The LPM allows to have an efficient way to approximate a Hölder spectrum and detects the non-concave part of this spectrum. Moreover, our implementation provides a method to detect the presence of several processes in a signal. Its development must be pursued. It would be interesting to mix several processes coming from practice (for example geometric

Brownian motion, Cascade of Mandelbrot, ...) and to apply our method. It will also be tested on real-life signals, for example on financial data feeds.

References

- [1] P. Abry, S. Jaffard, H. Wendt, A bridge between geometric measure theory and signal processing: Multifractal analysis, in: G. Karlheinz, M. Lacey, J. Ortega-Cerdà, M. Sodin (Eds.), Operator-Related Function Theory and Time-Frequency Analysis, 1–54.
- [2] A. Arneodo, G. Grasseau, M. Holschneider, Wavelet transform of multifractals, Phys. Rev. Lett. 61 (1988) 2281–2284.
- [3] J. Barral, S. Seuret, From multifractal measures to multifractal wavelet series, J. Fourier Anal. Appl. 11 (2005) 589–614.
- [4] F. Bastin, C. Esser, S. Jaffard, Large deviation spectra based on wavelet leaders, submitted.
- [5] I. Daubechies, Ten Lectures on Wavelets, CBMS-NSF Regional Conference Series in Applied Mathematics, 1992.
- [6] C. Esser, T. Kleyntssens, S. Nicolay, A multifractal formalism for non-concave and non-increasing spectra: the L^ν spaces approach, submitted.
- [7] S. Jaffard, The multifractal nature of Lévy processes, Probab. Theory Relat. Fields 114 (1999) 207–227.
- [8] J.-M. Aubry, S. Jaffard, Random wavelet series, Comm. Math. Phys. 227 (2002) 483–514.
- [9] S. Jaffard, Wavelet techniques in multifractal analysis, fractal geometry and applications: A jubilee of Benoit Mandelbrot, Proceedings of Symposia in Pure Mathematics 72 (2004) 91–151.
- [10] S. Jaffard, Beyond Besov spaces part 2: Oscillation spaces, Constr. Approx. 21 (2005) 29–61.
- [11] S. Jaffard, S. Nicolay, Pointwise smoothness of space-filling functions, Appl. Comput. Harmon. Anal. 26 (2009) 181–199.
- [12] T. Kleyntssens, C. Esser, S. Nicolay, A multifractal formalism based on the S^ν spaces: From theory to practice, submitted.
- [13] J.-F. Muzy, E. Bacry, A. Arneodo, Multifractal formalism for fractal signals: The structure function approach versus the wavelet-transform modulus-maxima method, Phys. Rev. E 47 (1993) 875–884.
- [14] G. Parisi, U. Frisch, On the singularity structure of fully developed turbulence, Turbulence and Predictability in Geophysical Fluid Dynamics (1985) 84–87.
- [15] S. Raible, Lévy processes in finance: Theory, numerics, and empirical facts, Ph.D. thesis (2000).
- [16] S. Seuret, Detecting and creating oscillations using multifractal, Math. Nachr. 279 (11) (2006) 1195–1211.